




## Deterioration effects of X-ray irradiation in artificially aged parchment

Fulvio Mercuri<sup>1</sup>, Cristina Cicero<sup>2,a</sup> , Stefano Paoloni<sup>1</sup>, Ugo Zammit<sup>1</sup>, Noemi Orazi<sup>1</sup>, Monia Vadrucci<sup>3,4</sup>, Leonardo Severini<sup>5</sup>, Claudia Mazzuca<sup>5</sup>

<sup>1</sup> Department of Industrial Engineering, University of Rome “Tor Vergata”, Via del Politecnico 1, 00133 Rome, Italy

<sup>2</sup> Department of Literary, Philosophical and Art History Studies, University of Rome “Tor Vergata”, Via Columbia 1, 00133 Rome, Italy

<sup>3</sup> Particle Accelerator for Medical Application Laboratory, Italian National Agency for New Technologies, Energy and Sustainable Economic Development (ENEA), Rome, Italy

<sup>4</sup> Science and Research Direction, Italian Space Agency (ASI), Via del Politecnico, 00133 Rome, Italy

<sup>5</sup> Department of Chemical Science and Technologies, University of Rome “Tor Vergata”, Via della Ricerca Scientifica, 00133 Rome, Italy

Received: 29 May 2023 / Accepted: 27 October 2023

© The Author(s) 2023

**Abstract** The effects of X-ray irradiation, a potential disinfection method, produced in parchment samples with different extent of artificial ageing have been investigated to analyse the possible superposition effects of the irradiation-induced damage with the existing ageing associated deterioration. The study was carried out in modern parchment samples in which different degrees of artificial ageing were induced by exposing them to severe hygro-thermal conditions for various durations. The aged samples were subsequently irradiated with increasing X-ray doses (350–4000 Gy). The consequent deterioration effects were analysed using light transmission analysis (LTA), attenuated total reflectance-Fourier transform infrared spectroscopy (ATR-FTIR) and fibre optic reflectance spectroscopy (FORS) in order to evaluate possible changes in, respectively, the hydro-thermal stability, the collagen protein structure (hydrolysis/denaturation) and the optical absorption/reflectance properties of the collagen protein. The results show increasing additional deterioration with irradiation dose for non-aged and moderately aged parchment, until damage saturation occurs for more intensively aged samples where no substantial additional deterioration is induced by the irradiation. The combined results indicate that the ageing produces the more substantial deterioration with respect to that induced by the irradiation treatment employed for disinfection purpose.

### 1 Introduction

Parchment has constituted one of the most important and widespread material used as writing support and for the manufacture of books [1] in the western world until the diffusion of paper. It is obtained from animal skin following a very complex manufacturing process aimed at obtaining a stable and resistant material able to last even for centuries [2, 3]. Because it is a collagen-based material, parchment is subject to degradation mainly due to the deteriorating agents present in the material and/or in the environment like acids, oxidizing agents, light and humidity. Owing to its nature, parchment is liable also to microbiological attacks, by bacteria or fungi. All these agents undermine the integrity of the parchment structure and therefore contribute to the degradation of its preservation state [4–8]. This not only jeopardizes the stability of the material but may also cause the loss of its written content like, for example, the case of the infection by purple spots [9–11]. Finally, microbiological-related deterioration turns out to be harmful also for the health of the personnel in contact with the artefact, namely librarians, archivists and scholars [9, 12–16].

Currently, several methods are used for the massive sterilization of library materials basically consisting in the fumigation with ethylene oxide or formaldehyde, or the irradiation of the samples with UV or gamma rays. The former, however, besides being toxic for humans and the natural environment, has been shown to enhance the possible attacks by mould [17]. The limitations to the use of ethylene oxide fumigation, indicated in recent years by the European Community [18–20], have prompted the scholars to find new approaches to the disinfection of this kind of cultural heritage (CH). Parchment is remarkably hygroscopic and cannot be wet-processed, so the use of some chemical agents, such as quaternary ammonium in aqueous solution, cannot be used in the case of collagen-based materials. In the spirit of a green approach to the restoration in general and to the disinfection in particular, and in an effort to reduce the use of chemicals, lately also the use of natural and biocompatible agents has been proposed. These include essential oils [18, 21] or plant extracts [22], though further studies are needed to evaluate their permanence and durability in relation to the thermo-hygro-metric conditions of the storage environment [18]. Gamma rays, on the other hand, have been applied in the disinfection treatment of large quantities of library and archive artefacts [23–32].

<sup>a</sup> e-mail: [cristina.cicero@uniroma2.it](mailto:cristina.cicero@uniroma2.it) (corresponding author)

Because of the safety requirements related to the access to gamma ray facilities, X-ray radiation has also been recently proposed as an alternative for disinfection treatments. In order to establish its possible effectiveness for this kind of application, it is necessary to determine the doses required for the infections curing in relation to the X-ray damage threshold in the material. In a more general context, the numerous works published on damage threshold in parchment witness that information on this issue are also of great interest to all those conservation scientists who use X-ray-based diagnostics, for example, fluorescence, micro-tomography, scattering and diffraction [33–35]. Studies to determine the doses necessary to cure infections in parchment have also been recently carried out in a dose range larger than those considered in the previously mentioned publications [36, 37]. The results showed that the complete removal of the biodegradation could be obtained with a single treatment with a minimum dose of 350 Gy [38], a value which was verified not to cause significant damage in sound modern parchment [39]. Such a damage threshold value was of the same order of magnitude as the one observed for ancient cotton paper [40, 41] and that which could be estimated from the threshold fluence values reported in ref. [42]. This is important in terms of the economic and environmental costs of the procedures particularly when considered in a perspective of the treatment of a large quantity of items.

In order to verify whether ageing effects could produce additional long-term deterioration effects in the irradiated parchment, artificial ageing under severe hygro-thermal conditions was induced after the irradiation, resulting in damage adding up on top of the irradiation-induced one basically independently of the irradiation dose [39]. The study of the X-ray irradiation effects was then carried out in historical biodeteriorated parchment so as to analyse both the possible damage induced by the radiation in the parchment as well as the extinction capability of the biodeteriogens. It was found that [43] the ageing-related deterioration, including that associated with the biological agents, proved to be of such an extent that no additional effects induced by the irradiation could be detected even at the largest employed dose, i.e. 4 kGy.

What now needs to be addressed is the effect induced by the X-ray irradiation in milder aged parchment and that is in samples with ageing-related deterioration levels intermediate between the modern parchment and the heavily aged ones. So, in this work the irradiation effects produced in parchment samples artificially aged to various stages of deterioration have been analysed. The study was carried out in modern parchment samples in which different degrees of artificial ageing were induced by exposing them to severe hygro-thermal conditions for various durations. The aged samples were subsequently irradiated with increasing X-ray doses. The deterioration effects associated both with the ageing and the X-ray irradiation were analysed using a variety of techniques. Light transmission analysis (LTA) was used to detect changes produced in the hydro-thermal stability of the collagen proteins [44]. Attenuated total reflectance-Fourier transform infrared (ATR-FTIR) spectroscopy was used to evaluate the changes induced in the collagen protein structure [45–47]. Fibre optic reflectance spectroscopy (FORS) was used to characterize the alterations induced in the optical absorption/reflectance properties of the processed parchment samples [48, 49].

## 2 Materials and methods

### 2.1 Parchment samples

Squares, of about  $20 \times 20 \text{ mm}^2$ , were cut out from the same area of an unwritten handmade modern goat parchment produced by the *National Research & Development Institute for Textiles and Leather of Rumania*, according to a traditional method. The samples were investigated before and after their processing consisting first in an artificial ageing procedure where the samples were kept in an environment at  $80^\circ \text{C}$  and at a relative humidity of 75% for durations of 2, 4, 8, 16 and 32 days to induce different levels of degradation. Thereafter, the samples were irradiated with different doses of X-rays in order to obtain different degree of radiation damage in the variously aged samples. All the investigations of the samples were completed within 60 days from the irradiation.

### 2.2 X-ray irradiation

In the present experiment, the treatments were performed in air, at room temperature and pressure conditions. The removable electrons to X-ray (REX) facility [36–39, 43] was used to perform the irradiation of the samples. It is a radiation source based on an electron accelerator designed and manufactured in the *ENEA* laboratories in Frascati for clinical and industrial applications. In the LINAC the electrons are accelerated up to an energy of 5 MeV. The beam is delivered in a micropulsed regime, with  $3.4 \mu\text{s}$  pulse length full width at half maximum (FWHM) and maximum beam current of 150 mA. The electron beam is extracted through a  $50\text{-}\mu\text{m}$  titanium exit window into a  $40 \times 40 \times 80 \text{ cm}^3$  lead-shielded irradiation chamber. This machine is able to deliver either electrons or X-rays exploiting bremsstrahlung process, through a removable electron to photon head conversion made of high atomic number materials, such as tungsten, gold, platinum and tantalum. The produced X-rays are characterized by a continuous spectral distribution of radiation that becomes more intense and shifted to larger frequencies with the increase in the energy of the incident electrons. In particular, in this study the spectrum obtained from tungsten has been used. The target is contained in a conical lead collimator (external diameter 30 mm) from which the X-ray beam emerges with a circular spot that spreads out in the irradiation chamber. The samples have been exposed a few centimetres in front of the X-ray source, to ensure the homogenous irradiation of the entire sample area. Given the density of the parchment, the X-ray beam could propagate through the sample thickness, thus delivering the dose in the entire sample volume. The radiation monitoring is carried out with an online system consisting of an ionization chamber with a

large spatial resolution. Gafchromic EBT3 dosimetry films, developed specifically for radiotherapy applications, have been used to monitor the dose distribution and spatial homogeneity of the radiation beams set up for the treatment campaigns, and Gafchromic HD-V2 high-dose dosimetry films have been used to intercalibrate the ionization chamber dosimetry up to 1000 Gy. The process control procedures have been defined so as to accurately deliver the specified dose to each of the samples. Treatments are operated at 0.35 mGy/s with an adsorbed dose error less of 0.5%.

### 2.3 LTA

LTA is a technique which has shown to be effective in evaluating the hydro-thermal stability of the collagen protein in various substrates obtained from animal skin like parchment, leather and alum-tawed skin by determining, in full hydration conditions, their denaturation temperature  $T_d$ , whose value can be related to the deterioration degree of the material [44]. A typically 1 mm<sup>2</sup> sample area is pulped with a blade to obtain a suspension of fibres in water and therefore in condition of saturated hydration. It is contained in a 0.1-mm-thick quartz cell whose temperature is varied in an oven with a substantially constant temperature rate of about 1 °C/min. During the measurements, performed from room temperature up to 90 °C, the light from a He–Ne laser beam is directed across the sample to probe its scattering capability which, during the hydro-thermal denaturation of the fibres, becomes substantially reduced, thus yielding an increase of the light transmitted through the sample. Such light is collected by a lens and then focused onto a photodiode. The transmitted light signal is recorded as a function of temperature to evaluate  $T_d$ , which is taken as the temperature at which the maximum rate of change of the transmitted light, and therefore, of the denaturation activity, occurs. The temperature derivative of the transmission data will thus show a peaked feature whose maximum will occur at  $T_d$ . The larger will be the denaturation temperature, the better the chemical integrity of the collagen fibres and, therefore, the sample preservation condition [44]. The reported  $T_d$  values correspond to averages of three different measurements.

### 2.4 ATR-FTIR spectroscopy

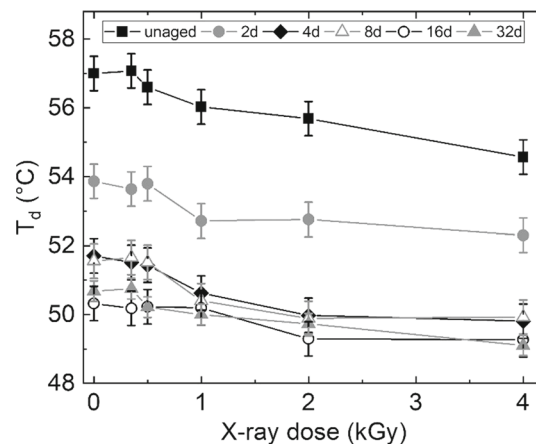
FTIR absorption spectra were collected using the Thermo-Scientific instrument, model Is50, in the attenuated total reflectance (ATR) mode using a single reflection diamond cell. The spectra were recorded between 4000 and 750 cm<sup>-1</sup>, averaging over 32 scans with a resolution of 2 cm<sup>-1</sup>. All experiments were carried out in triplicate, yielding consistent and reproducible results. Spectra profile deconvolution was performed in the 1360–1800 cm<sup>-1</sup> region on normalized absorbance ATR-FTIR spectra assuming Voigt bands of FWHM of 25 cm<sup>-1</sup> maximum, using the OMNIC software. The baseline-corrected spectra were normalized to the highest band (Amide I), so that the absorbance of the highest peak is equal to 1.0. Spectra are baselined where no absorbance peaks are present (1950 cm<sup>-1</sup>).

The ATR-FTIR investigations have been carried out to detect possible deterioration effects, borne by collagen molecules in the parchments, induced by ageing and X-ray exposure. Indeed, ATR-FTIR spectroscopy allows the monitoring of the changes in the proteins secondary structures, in a non-destructive way, through the analysis of Amide I and Amide II bands, which are most commonly used in conformational protein studies (i.e. for monitoring protein denaturation and/or aggregation processes) [50, 51]. In particular, the Amide I band is found between 1700 and 1600 cm<sup>-1</sup>, and it is mainly associated with the C=O stretching vibration belonging to polypeptide chain and it is sensitive to local structural order. Such a band is composed of different secondary structures centred at different frequencies. The Amide II band occurs between 1570 and 1500 cm<sup>-1</sup> and is originated mainly from NH in-plane bending and CN stretching. By exploiting the study of the intensity ratio of these vibrational bands ( $I_{\text{AmideI}}/I_{\text{AmideII}}$ ), it is possible to evaluate the degree of hydrolysis of the parchment collagen protein. An increase in the value of this ratio indicates an increase in the degree of hydrolysis that can take place in the sample due to increased amounts of water content [52]. Moreover, the relative distance between the Amide I and II bands ( $\Delta\nu$ ) is a good indicator of the conservation state of the parchment. In particular, an increase of the value of this parameter indicates a greater denaturation/gelatinization of the collagen triple helix in the sample [52].

### 2.5 FORS

FORS is a non-destructive technique which can be used for in situ investigation of CH. It can provide researchers and conservators with data useful for the spectral analysis of colour and its possible variation. In this work, the reflectance spectra have been collected in the 400–900 nm range by means of a portable *StellarNet GREEN-Wave* spectrometer using a D65 illuminant. The instrument consists of a fibre coupled optical source and the measurements are performed by collecting the diffuse reflected light from a sample area of about 1 cm<sup>2</sup> with the aid of an integrating sphere (*StellarNet FORS Systems*, 2021). Data refer to five averages made on every investigate sample. The calibration of the system has been performed using a reference sample certified to reflect more than 97% of the incident light in the range 300–1700 nm. In this work, the FORS evaluations were performed to investigate the changes induced in the absorption/reflection properties of the parchment associated with the deterioration induced by the ageing and the X-ray irradiation.

**Fig. 1** Parchment denaturation temperature  $T_d$  versus irradiation dose in samples artificially aged for increasing number of days. The vertical lines indicate the maximum uncertainty associated to the measured  $T_d$  values



### 3 Results and discussion

#### 3.1 LTA results

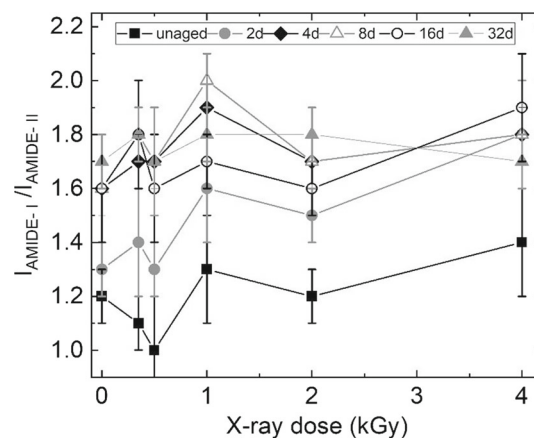
LTA has been performed in all the samples and the changes obtained in the denaturation temperature,  $T_d$ , analysed in order to evaluate to what extent the artificial ageing and irradiation they were subject to induced damage in the parchment proteins. The results are displayed in Fig. 1 where the  $T_d$  values are shown as a function of the irradiation dose for all the differently aged samples. For the unaged samples, the  $T_d$  values are the largest for all the irradiation dose values. No substantial change in the values is shown up to the irradiation dose of 350 Gy, while, for larger doses, the general trend in the  $T_d$  values shows a progressive slow decrease even though many of the decreasing values fall within the maximum uncertainty range of the data. The observed trend is in agreement with an earlier work [38] which showed that, in unaged modern parchment and for large enough doses, the irradiation process can produce a progressive reduction of the stability of the collagen until a saturation tendency of the  $T_d$  values is achieved. Trends very similar to those obtained for the unaged sample are obtained also for the samples artificially aged for 2 and 4 days, but with progressively lower values of  $T_d$  at all irradiation doses. This is due to the progressively larger ageing associated damage, on top of which that associated to the irradiation cumulates. This is true up to the ageing duration of 4 days, since only minor additional reduction in the  $T_d$  values is observed for longer duration of the artificial ageing, indicating that the cumulative effect of the ageing and the irradiation associated damage tends to saturate with increasing ageing. It is also evident from the data that it is the ageing that produces the more substantial deterioration with respect to that induced by the irradiation. However, at the present artificial ageing conditions, for durations of 8 days and longer, the correspondingly induced deterioration tends to saturate and very small additional changes in  $T_d$  are obtained following the irradiation process even with increasing dose values. This is in agreement with the results previously obtained in a heavily naturally deteriorated parchment sample [43] where no systematic change in  $T_d$  with increasing irradiation dose could be detected. It is also interesting to point out that, while the results in Fig. 1 show that the irradiation process does not produce any substantial additional deterioration with respect to that induced by the artificial ageing lasting 32 days, the two kinds of deterioration do sum up when the order of the two processes is reversed. In fact, in ref. 38 it was shown that artificial ageing for 32 days of a modern parchment sample that had previously been irradiated produced a substantial additional lowering of  $T_d$  with respect to that induced by the irradiation process for all the employed doses. These results can be explained if one considers that the damage produced by the irradiation is likely of a different nature and of a less severe extent than that produced by the ageing so that when severe ageing is induced in an irradiated sample the two deteriorogenic effects can add up, while irradiation of an already severely damaged (aged) parchment does not produce substantial additional deterioration.

#### 3.2 ATR-FTIR spectroscopy results

ATR-FTIR spectroscopy has been employed to detect possible damage to the collagen molecules due to artificial ageing and X-ray irradiation, individually or concurrently applied. Before the measurements, all the samples were conditioned for 1 week under the same conditions of temperature ( $20 \pm 0.5$  °C) and relative humidity ( $45 \pm 2\%$ ), as established by the ISO 1 standard.

In Fig. 2 we report the ratio of the intensities of the Amide I to Amide II bands as a function of the irradiation dose for the differently aged samples, similarly to what reported in Fig. 1 for the protein denaturation temperature, where increases of such ratio would witness an increase of the degree of hydrolysis of the proteins structure. The results were obtained from the corresponding absorbance spectra some of which are reported in the supplementary material (Fig. SI 1 and SI 2). The obtained spectra were baselined at  $1950 \text{ cm}^{-1}$ , where no absorbance peaks are present, and thereafter normalized to the largest band (Amide I) maximum value so that the absorbance value at that peak is 1.

**Fig. 2** Amide I–Amide II intensity ratio versus irradiation dose in samples artificially aged for increasing number of days



The trend of the changes induced by the irradiation and ageing of the samples closely resembles that reported in Fig. 1 for the  $T_d$  values. In fact, for the unaged samples the values of the ratio are the smallest at all the irradiation doses. Moreover, though the changes of the values representing the trend sometimes fall within the maximum uncertainty range of the data, because of the large value of the uncertainty, there is a general trend for the average values for each sample of the intensity ratio to increase with increasing irradiation dose. This also points to a progressive increase of damage with irradiation dose as implied by the changes in the  $T_d$  values displayed in Fig. 1. Trends very similar to those obtained for the unaged sample are obtained also for the samples artificially aged for 2 and 4 days, but starting from progressively larger values of the Amide I to Amide II intensity ratio. This is because of the larger initial extent of the hydrolysis, induced by the increasing ageing, on top of which the damage induced by the irradiation then overlaps. Moreover, even in these results, it is shown that it is the ageing which produces the more substantial deterioration, with respect to that induced by the irradiation, and, for ageing durations larger than 4 days, the deterioration levels tend to saturate and very small additional changes are obtained with irradiation at all doses, similarly to the trend shown in Fig. 1. Finally, even in the case of the intensity ratio results, very small additional changes are obtained for increasing irradiation dose in the sample aged for the longest duration. ATR-FTIR results thus confirm the damage trends shown by the LTA analysis. It must finally be remarked that the relative distance between the Amides I and II bands was shown to remain practically unchanged ( $\Delta\nu \sim 89 \text{ cm}^{-1}$ ) following the artificial ageing and the irradiation process, indicating that the triple helical structure of the collagen molecules is substantially maintained following the correspondingly induced deterioration. These results demonstrate that the progressive partial destructuring and/or hydrolysis of the protein occurs without affecting substantially the triple helical structure [53, 54].

The extent of the damage induced by the artificial ageing under the conditions adopted in the present work can be compared with that found in naturally aged parchment reported in a previous work [43] for naturally deteriorated ancient parchment samples. In the case of the present samples, the value of the intensity ratio ranges between  $1.2 \pm 0.1$  and  $1.7 \pm 0.1$  for unaged and artificially aged sample, respectively, while that of a naturally aged ancient parchment sample investigated in the previous work was  $3.0 \pm 0.1$ . Furthermore, the relative distance between the Amides I and II bands was about  $89 \text{ cm}^{-1}$  for the present samples and  $93 \text{ cm}^{-1}$  for the ancient one, thus emphasizing an evident denaturation and/or gelatinization of the collagen triple helix occurring only in the latter [53]. The considerable larger degree of deterioration of the naturally aged ancient parchment with respect to the modern artificially aged ones is thus evident, bearing in mind that the former, beside the effects of the naturally occurring structural deterioration was subject also to considerable bacterial attack. These results are consistent also with the progressive decreasing dependence of the induced deterioration from the irradiation dose found in the modern parchment samples artificially aged for the longest durations as shown in Figs. 1 and 2. In fact, no such dose dependence could be found in the substantially more deteriorated naturally aged sample [43].

Because of the sensitivity of the Amide I (and, to a smaller extent, of the Amide II) band peak position to the presence of several secondary structures, the energy position of such components was evaluated by deconvolving them from the overall band profile. Indeed, the Amide I band is centred at  $1631 \text{ cm}^{-1}$ , displaying three components at  $1690 \text{ cm}^{-1}$ ,  $1660 \text{ cm}^{-1}$  and  $1630 \text{ cm}^{-1}$  assignable to carbonyl stretching in different situations following acid side-chains interactions, within the  $\alpha$ -helix structures and in disordered conformations, respectively. In the latter case, carbonyl is therefore more prone to interact with water by means of hydrogen bonds [55, 56]. In this way, it is possible to analyse the effect of the various procedures the parchment is subject to on each of the specific molecular changes. We first report the results concerning the changes induced by the increasing X-ray irradiation dose. In Fig. 3 the area beneath each secondary structure is reported in the case of the unaged sample which the previous results showed to be most sensitive to the irradiation treatments. It can be seen that the intensity of all the probed sub-bands remains substantially unchanged with the increasing dose, thus showing that this specific kind of analysis of the FTIR-ATR data prove to be less sensitive to the effects of the increasing dose with respect to that implying the ratio of the Amide I–Amide II bands. Figure 4 reports the Amide I sub-bands analysis obtained in the parchment with the largest extent of initial ageing. Even in this case the results prove to be insensitive to the

**Fig. 3** Relative area values for the Amide I components, deconvolved from the overall profile of the band, versus irradiation doses for the unaged sample

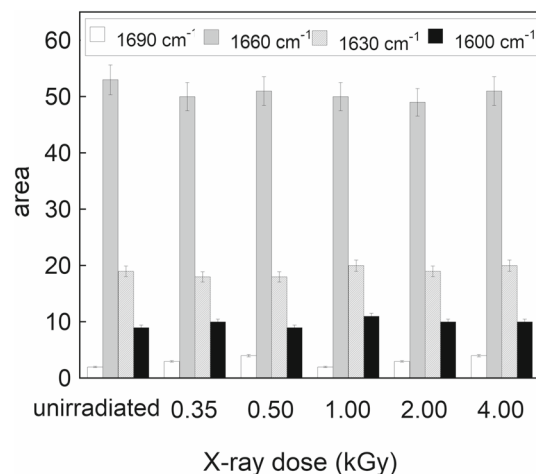
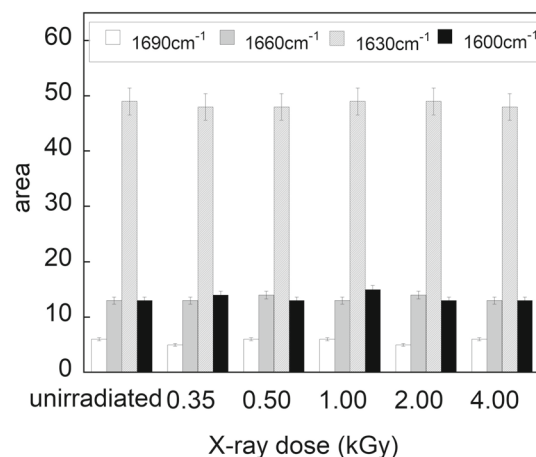


**Fig. 4** Relative area values for the Amide I components, deconvolved from the overall profile of the band, versus irradiation doses for the 32 days aged sample



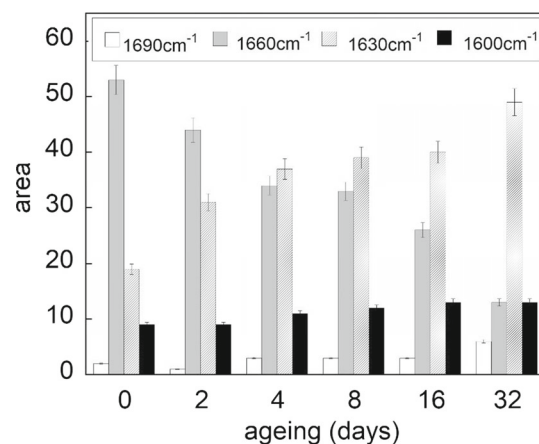
increasing dose values, not surprisingly considering the lower sensitivity to such an effect for this sample witnessed by the results in Figs. 1 and 2.

Finally, in Fig. 5 we report the Amide I sub-bands analysis obtained in the parchments subject only to the increasing ageing effects given its major role in eventually overshadowing that induced by the irradiation. It is shown that the area beneath each secondary structure is reported as a function of the ageing for the non-irradiated samples. It is shown that the intensity of the 1660 cm<sup>-1</sup> sub-band ( $\alpha$ -helix) decreases with ageing, while the area of 1630 cm<sup>-1</sup> sub-band (disordered conformation) undergoes the opposite variation, indicating a progressive destructuring of the protein and therefore some possible local uncoiling of the helices which, however, could not be detected from the analysis of the Amide I–Amide II bands distance, as pointed out earlier on. It is also possible to identify an increase in the contribution of the acid side-chain interactions (1690 cm<sup>-1</sup>) and in the bound water content (1600 cm<sup>-1</sup>) which become more significant with ageing. These results are consistent with the overall progressive increase of the degree of hydrolysis with ageing witnessed in Fig. 2 [52–57]. Further confirmation of the deterioration associated with the ageing has been provided by the study of the 1745 cm<sup>-1</sup> band, attributed to carboxyl groups (like esters), and that at 1795 cm<sup>-1</sup>, associated with the C=O stretching of acyl halide or carbonates, probably resulted due to collagen oxidation/cross-linking (data not shown). Their intensities increase with the ageing days, pointing out an increase in the deterioration [58].

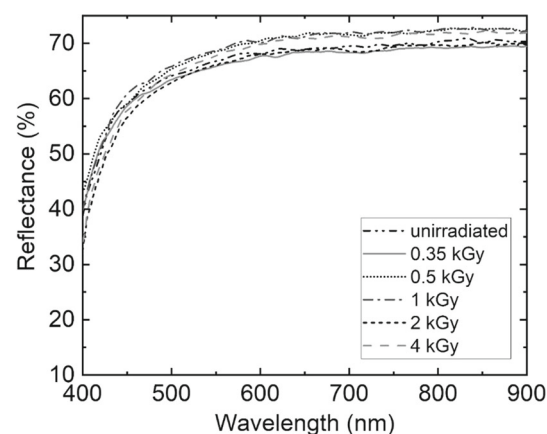
### 3.3 FORS results

Figure 6 reports the diffuse reflectance spectra in the visible-near infrared (NIR) range of the non-aged samples irradiated with increasing X-ray dose values, to probe the effect of the irradiation damage alone. Also for this technique, the results obtained for the unaged sample are reported since it is the sample where the previous investigations showed the largest sensitivity to irradiation-induced damage. It is observed that only a slight increase occurs in the measured reflectance all over the investigated range with no change in the spectral relative features. This indicates that the spectral position of the various absorption bands, characteristic of parchment, does not substantially change with irradiation. These include those characteristic of the amide structure and can be identified by the  $\pi \rightarrow \pi^*$  and  $n \rightarrow \pi^*$  electronic transitions occurring in the C=O, NH and CONH groups in the collagen molecules [58, 59]. Such transitions in sound parchment affect the absorption in the 250–400 nm spectral range [58] and may be shifted to

**Fig. 5** Relative area values for the Amide I components, deconvolved from the overall profile of the band, versus ageing for the unirradiated sample



**Fig. 6** Diffuse reflectance spectra for unaged parchment samples irradiated with increasing X-ray dose

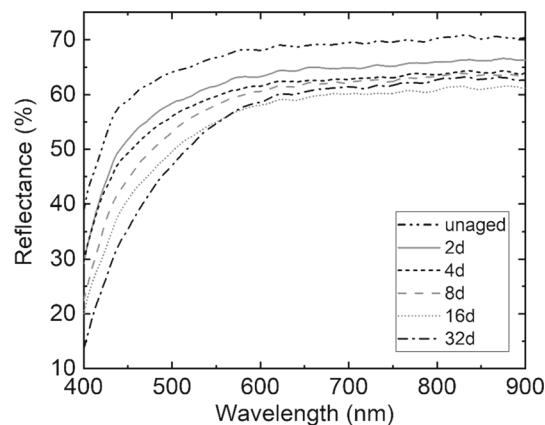


longer wavelength by the degradation of the parchment such as that induced by ageing [58, 59]. So, it is shown that even the FORS analysis is not sensitive enough to discriminate between the effects produced by the increasing irradiation dose, once again unlike the case of the results reported in Figs. 1 and 2.

Finally, the results concerning the effects of the damage induced by the ageing alone are reported in Fig. 7. With increasing artificial ageing duration, the shoulder feature in the shorter wavelength visible region is shown to shift to longer wavelength, indicating an increase of the absorption in the shorter wavelength range. Moreover, a progressive decrease of the reflectance values all over the investigated range is also observed. Thus, ageing causes a progressive shift to longer wavelength of the previously mentioned absorption bands, revealing structures with extended conjugation resulting most likely from oxidation of organic acids existent in the system, as pointed out by the FTIR results, and also as previously observed in naturally aged parchments [58]. As a result, the absorption edge shifts progressively to values even above 500 nm, inducing the parchment to acquire a light yellow coloration. This is evident also in the corresponding variation of the colorimetric coordinates, also reported in the supplementary information (SI Table 1), where the value of the *b* colorimetric coordinate progressively increases with ageing, denoting a shift towards a yellow coloration. No significant change in the colorimetric coordinates could be detected induced by the increasing irradiation dose.

A final remark should concern the different sensitivities of the various analytical techniques employed for the present study. The LTA data are the ones which show the greatest discrimination between the results obtained for the different irradiation dose, denoting the largest sensitivity to this variable. The results of the analysis of the Amide I–Amide II bands ratio also proved sensitive to such a parameter but to a lesser extent. A possible explanation could concern the different parchment volume probed by the two techniques. LTA involves transmission measurements and therefore probes the entire thickness of the investigated fibres sample (100  $\mu\text{m}$ ), while ATR-FTIR investigates very superficial layers of the parchment. This is in part true also for the FORS characterizations where reflectance measurements at a highly scattering surface are involved. Moreover, the LTA measurements are performed with the sample in water whose presence could additionally weaken the molecular bonds which may have been deteriorated by the irradiation/ageing effects, thus amplifying the original deterioration effect.

**Fig. 7** Diffuse reflectance spectra for unirradiated parchment samples artificially aged for increasing number of days



#### 4 Conclusions

Exposure of parchment to X-rays, a treatment that could be used for its disinfection, was studied in samples undergoing accelerated ageing to analyse the superposition effects of the irradiation-induced damage with that previously caused by non-adequate hygro-thermal conditions.

The study was carried out in modern parchment samples in which different extent of artificial ageing was induced by exposing them to severe hygro-thermal conditions for various durations. The samples were subsequently irradiated with increasing X-ray doses. The consequent deterioration effects were analysed using a variety of techniques, namely light transmission analysis, attenuated total reflectance-Fourier transform infrared spectroscopy and fibre optic reflectance spectroscopy. The LTA analysis indicated that the increased deterioration was associated with a reduction of the collagen denaturation temperature, and that it is the ageing that produces the more substantial deterioration with respect to that induced by the irradiation. Moreover, the irradiation damage adds up on top of that associated with ageing until, for long-enough artificial ageing treatments, the deterioration tends to saturate and very small additional changes are obtained with irradiation. The same damage trend is shown by the ATR-FTIR results obtained from the analysis of the Amide I–Amide II bands intensity ratio, which reflects the degree of hydrolysis of the parchment collagen proteins. The analysis of the Amide I band components, which can be deconvolved from the overall band profile, confirms that it is the ageing that mainly contributes to the parchment deterioration, causing a decrease of the  $\alpha$ -helix sub-band intensity, an increase of the destructuring of the protein and an increase in the acid side-chain interactions and in the bound water content. This is consistent with the overall progressive increase of the protein hydrolysis. Finally, the ageing produces a progressive red-shift of the absorption bands observed in the UV–VIS spectral range.

**Supplementary Information** The online version contains supplementary material available at <https://doi.org/10.1140/epjp/s13360-023-04635-5>.

**Acknowledgements** The parchment employed in this study has been produced, following traditional methods, by *The National Research & Development Institute for Textiles and Leather*, ICPI Division, Ion Minulescu Street no. 93, 031215 Bucharest, Romania. C.C. acknowledges the co-funding of the European Union FSE RE-ACT-EU-PON Ricerca e Innovazione 2014–2020, DM 1062/2021.

**Author contributions** FM and UZ designed the study and with CC contributed to the conception of the experimental campaigns. MV performed the irradiation tests; CM and LS performed the FTIR spectroscopy; FM, CC and SP performed the LTA analysis; UZ and NO performed the colorimetric analysis; UZ wrote the first draft of the manuscript; all authors contributed to manuscript revision, read and approved the submitted version.

**Funding** Open access funding provided by Università degli Studi di Roma Tor Vergata within the CRUI-CARE Agreement.

**Data Availability Statement** Data will be made available on reasonable request. This manuscript has associated data in a data repository. [Authors' comment: Supplementary data include some of the obtained ATR-FTIR absorption spectra and colorimetric analysis results.]

#### Declarations

**Conflict of interest** The authors declare that the research was conducted in the absence of any commercial or financial relationships that could be construed as a potential conflict of interest.

**Open Access** This article is licensed under a Creative Commons Attribution 4.0 International License, which permits use, sharing, adaptation, distribution and reproduction in any medium or format, as long as you give appropriate credit to the original author(s) and the source, provide a link to the Creative Commons licence, and indicate if changes were made. The images or other third party material in this article are included in the article's Creative Commons licence, unless indicated otherwise in a credit line to the material. If material is not included in the article's Creative Commons licence and your intended use is not permitted by statutory regulation or exceeds the permitted use, you will need to obtain permission directly from the copyright holder. To view a copy of this licence, visit <http://creativecommons.org/licenses/by/4.0/>.



## References

1. M.L. Agati, *The Manuscript Book, a Compendium of Codicology*, 1st edn. (L'Erma di Bretschneider, Roma, 2017)
2. C. Clarkson, *Pap. Conserv.* **16**, 5 (1992). <https://doi.org/10.1080/03094227.1992.9638571>
3. B. Haines, in *Conservation of Leather and Related Materials*. ed. by M. Kite, R. Thomson (Elsevier, Oxford, 2006), pp.198–199
4. C. Kennedy, T. Wess, *Restaurator* (2003). <https://doi.org/10.1515/REST.2003.61>
5. M. Kite, R. Thomson, *Conservation of Leather and Related Materials*, 1st edn. (Routledge, London, 2005)
6. E.F. Hansen, S.N. Lee, H. Sobel, *JAIC* **31**, 3 (1992). <https://doi.org/10.1179/019713692806066600>
7. M.C. Area, H. Cheradame, *BioResources* **6**, 4 (2011)
8. J. Havermans, P. Marres, P. Defize, *Restaurator* **20**(1), 48–55 (1999). <https://doi.org/10.1515/rest.1999.20.1.48>
9. L. Migliore, M.C. Thaller, G. Vendittozzi, A.Y. Mejia, F. Mercuri, S. Orlanducci, A. Rubecchini, *Sci. Rep.* **7**, 9521 (2017)
10. G. Piñar, K. Sterflinger, F. Pinzari, *Environ. Microbiol.* **17**(2), 427–443 (2015)
11. F. Gallo, A. Strzelczyk, *Bollett. Ist. Centr. Patologia Libro “Alfonso Gallo”* **30**(1/2), 71–87 (1971)
12. R. Craig, *Pap. Conserv.* (1986). <https://doi.org/10.1080/03094227.1986.9638528>
13. F. Pinzari, V. Cialei, G. Piñar, in *Historical Technology, Materials and Conservation: SEM and Microanalysis*. ed. by N. Meeks, C. Cartwright, A. Meek, A. Mongiatti (Archetype Publications, London, 2012), pp.93–99
14. G. Piñar, K. Sterflinger, J. Etenauer, A. Quandt, F. Pinzari, *Microb. Ecol.* **69**, 118–134 (2015). <https://doi.org/10.1007/s00248-014-0481-7>
15. C. Cicero, F. Pinzari, F. Mercuri, *Int. Biodeterior. Biodegrad.* **184**, 76–82 (2018). <https://doi.org/10.1016/j.ibiod.2018.08.007>
16. L. Migliore, N. Perini, F. Mercuri, S. Orlanducci, A. Rubecchini, M.C. Thaller, *Sci. Rep.* **9**, 1623 (2019). <https://doi.org/10.1038/s41598-018-37651-y>
17. N. Valentin, *Pap. Conserv.* **10**, 1 (1986). <https://doi.org/10.1080/03094227.1986.9638530>
18. K. Pietrzak, A. Otlewska, D. Danielewicz, K. Dybka, D. Pangallo, L. Kraková, A. Puškárová, M. Bučková, V. Scholtz, M. Ďurovič, B. Surma-Ślusarska, K. Demnerová, B. Gutarowska, *J. Cult. Herit.* **24**, 69–77 (2017). <https://doi.org/10.1016/j.culher.2016.10.011>
19. International Agency on Research on Cancer, *IARC Monographs on the Evaluation of Carcinogenic Risks to Humans, Volume 88, Formaldehyde, 2-Butoxyethanol and 1-tert-Butoxypropan-2-ol* (World Health Organization, Lyon, 2006)
20. International Agency on Research on Cancer, *IARC Monographs on the Evaluation of Carcinogenic Risks to Humans, Volume 97, 1,3-Butadiene, EthyleneOxide and Vinyl Halides (Vinyl Fluoride Vinyl Chloride and Vinyl Bromide)* (World Health Organization, Lyon, 2008)
21. S. Macedo-Arantes, A. Piçarra, A.T. Caldeira, A.E. Candeias, M.R. Martins, *Eur. Phys. J. Plus* **136**, 1106 (2021). <https://doi.org/10.1140/epjp/s13360-021-02018-2>
22. S. Ismael, A. Omar, M. Maher, *Heritage* (2021). <https://doi.org/10.3390/heritage4030140>
23. M.C. Area, A.M. Calvo, F.E. Felissia, A. Docters, M.V. Miranda, *Radiat. Phys. Chem.* **96**, 217–222 (2014). <https://doi.org/10.1016/j.radphyschem.2013.10.004>
24. R. Kowalik, *Restaurator* (1980). <https://doi.org/10.1515/rest.1980.4.3-4.135>
25. M.G. Adamo, M. Giovannotti, G. Magaouda, M. Plossi Zappalà, F. Rocchetti, G. Rossi, *Restaurator* (1998). <https://doi.org/10.1515/rest.1998.19.1.41>
26. M.G. Adamo, G. Magaouda, G. Martinelli, M. Plossi Zappalà, F. Rocchetti, F. Savagnone, *Restaurator* (2001). <https://doi.org/10.1515/REST.2001.107>
27. M. Da Silva, A.M.L. Moraes, M.M. Nishikawa, M.J.A. Gatti, M.A. Vallim de Alencar, L.E. Brandão, A. Nóbrega, *Int. Biodeterior. Biodegrad.* **57**, 163–167 (2006). <https://doi.org/10.1016/j.ibiod.2006.02.003>
28. G. Magaouda, *J. Cult. Herit.* **5**, 113–118 (2014). <https://doi.org/10.1016/j.culher.2003.07.003>
29. M.L. Otero D'Almeida, P. Medeiros Barbosa, M.F. Guerra Boaratti, S.I. Borrelly, *Radiat. Phys. Chem.* **78**, 489–492 (2009). <https://doi.org/10.1016/j.radphyschem.2009.03.032>
30. C. Sendrea, E. Badea, I. Stănculescu, L. Miu, H. Iovu, *Revista de Pielarie Incaltaminte* **15**, 139–150 (2015)
31. C. Sendrea, C. Carsote, M. Radu, E. Badea, L. Miu, *Rev. Chim.* **68**, 1535–1538 (2017)
32. I. Nunes, N. Mesquita, S. CaboVerde, M. Trigo, A. Ferreira, M.M. Carolino, A. Portugal, M.L. Botelho, *Radiat. Phys. Chem.* **81**, 1943–1946 (2012)
33. K. Patten, L. Gonzalez, C. Kennedy, D. Mills, G. Davis, T. Wess, *Herit. Sci.* **1**, 22 (2013). <https://doi.org/10.1186/2050-7445-1-22>
34. M. Moini, C.M. Rollman, L. Bertrand, *Anal. Chem.* **86**, 9417–9422 (2014). <https://doi.org/10.1021/ac502854d>
35. L. Bertrand, S. Schöder, D. Anglos, M.B.H. Breese, K. Janssens, M. Moini, A. Simon, *TRAC* **66**, 128–145 (2015). <https://doi.org/10.1016/j.trac.2014.10.005>
36. M. Vadrucchi, F. Borgognoni, C. Cicero, N. Perini, L. Migliore, F. Mercuri, N. Orazi, A. Rubecchini, *Appl. Radiat. Isot.* **149**, 159–164 (2019). <https://doi.org/10.1016/j.apradiso.2019.04.021>
37. M. Vadrucchi, G. De Bellis, C. Mazzuca, F. Mercuri, F. Borgognoni, E. Schifano, D. Uccelletti, C. Cicero, *Front. Mater.* (2020). <https://doi.org/10.3389/fmats.2020.00021>
38. M. Vadrucchi, C. Cicero, P. Parisse, L. Casalis, G. De Bellis, *Appl. Surf. Sci.* (2020). <https://doi.org/10.1016/j.apsusc.2020.145881>
39. M. Vadrucchi, C. Cicero, C. Mazzuca, F. Mercuri, M. Missori, N. Orazi, L. Severini, U. Zammit, *Eur. Phys. J. Plus* **136**, 873 (2021). <https://doi.org/10.1140/epjp/s13360-021-01766-5>
40. A. Gimat, S. Schöder, M. Thoury, M. Missori, S. Paris-Lacombe, A.-L. Dupont, *Biomacromolecules* **21**, 2795–2807 (2020). <https://doi.org/10.1021/acs.biomac.0c00512>
41. A. Gimat, S. Schöder, M. Thoury, A.-L. Dupont, *Cellulose* **29**, 4347–4364 (2022). <https://doi.org/10.1007/s10570-022-04552-3>
42. G. Young, *Effect of High Flux X-radiation on Parchment (No. Report No. Proteus 92195)* (Canadian Conservation Institute, Ottawa, 2005)
43. M. Vadrucchi, C. Cicero, C. Mazzuca, L. Severini, D. Uccelletti, E. Schifano, F. Mercuri, U. Zammit, N. Orazi, F. D'Amico, P. Parisse, *Heritage* **6**, 1308–1324 (2023). <https://doi.org/10.3390/heritage6020072>
44. C. Cicero, F. Mercuri, S. Paoloni, N. Orazi, U. Zammit, C. Glorieux, J. Thoen, *Thermochim. Acta* **676**, 263–270 (2019). <https://doi.org/10.1016/j.tca.2019.05.007>
45. B. De Campos Vidal, M.L.S. Mello, *Micron* **42**, 283–289 (2011). <https://doi.org/10.1016/j.micron.2010.09.010>
46. K. Schwing, M. Gerhards, *Int. Rev. Phys. Chem.* **35**, 569–677 (2016). <https://doi.org/10.1080/0144235X.2016.1229331>
47. S.A. Asher, M. Ludwig, C.R. Johnson, *J. Am. Chem. Soc.* **108**, 3186–3197 (1986). <https://doi.org/10.1021/ja00272a005>
48. E. Ganz, H.K.A. Pauli, *Appl. Opt.* **34**, 2998–2999 (1995). <https://doi.org/10.1364/AO.34.002998>
49. C. Oleari, *Misurare il colore*, 1st edn. (Hoepli, Milano, 2008)
50. P. Nebojsa, K.A. Nils, O. Ragni, K. Achim, *J. Agric. Food Chem.* **59**, 10052–10061 (2011). <https://doi.org/10.1021/jf201578b>
51. B. Shivu, S. Seshadri, J. Li, K.A. Oberg, V.N. Uversky, A.L. Fink, *Biochemistry* **52**, 5176–5183 (2013). <https://doi.org/10.1021/bi400625v>
52. V. Plavan, M. Giurginca, P. Budrugaec, M. Vilsan, L. Miu, *Rev. Chim.* **61**, 627–631 (2010)
53. C.A. Miles, A. Sionkowska, S.L. Hulin, T.J. Sims, N.C. Avery, A.J. Bailey, *J. Biol. Chem.* **275**, 33014–33020 (2000)
54. F. Cappa, I. Paganoni, C. Carsote, E. Badea, M. Schreiner, *Herit. Sci.* **8**, 15 (2020). <https://doi.org/10.1186/s40494-020-0353-z>

55. K.J. Payne, A. Veis, *Biopolymers* **27**, n1749-1760 (1988). <https://doi.org/10.1002/bip.360271105>
56. P.I. Haris, D. Chapman, *Biopolymers* **37**, 251–263 (1995). <https://doi.org/10.1002/bip.360370404>
57. G. Ebersbach, M. Kopecká, R. Prokeš, J. Příhoda, *Herit. Sci.* **7**, 26 (2019). <https://doi.org/10.1186/s40494-019-0269-7>
58. L. Miu, M. Giurginca, A. Meghea, *Sci. Bull. B Chem. Mater. Sci. UPB* **70**, 51–56 (2008)
59. E. Badea, L. Miu, P. Budrugaec, M. Giurginca, A. Mašić, N. Badea, G. DellaGatta, *J. Therm. Anal.* **91**, 17–27 (2008). <https://doi.org/10.1007/s10973-007-8513-x>